Model for the vibrational spectra of B_2O_3-xLi_2O

Rafael A. Barrio
Instituto de Física, Universidad Nacional Autónoma de México, Apartado Postal 20-364, 01000 México, Distrito Federal, Mexico

Fray de Landa Castillo-Alvarado
Escuela Superior de Física y Matemáticas, Instituto Politécnico Nacional, Edificio 9 Unidad Profesional Adolfo López Mateos, 07738 México, Distrito Federal, Mexico

(Received 26 May 1992)

A nested coherent-potential approximation in the Bethe lattice is used to model the vibrational spectra in the vitreous compound B_2O_3-xLi_2O. A local-polarizability model is applied to calculate the Raman and infrared activity of the modes, and the results are compared with experimental data. The agreement is not complete due to the presence of rather complicated local configurations in the glass, as boroxol rings, diborate and tetraborate groups, not taken into account in the theory. However, this calculation is useful to identify the main features of the experimental spectra, and to corroborate the hypothesis of structural changes that occur when doping the pure boron oxide with an alkali-metal oxide.

I. INTRODUCTION

Pure vitreous B_2O_3 is a fascinating transparent material with numerous technological applications. Its structure has been a matter of debate, although by now there seems to be a universal acceptance of the original proposal that nearly all the boron atoms belong to planar hexagonal "boroxol" rings.[1] Each boron atom is at the center of an equilateral triangle of oxygen atoms, as revealed by NMR studies,[2] and the oxygen atoms form bridges between the borons. In the boroxol rings the B-O-B angle is $2\pi/3$ and in the bridges is $\approx 130°$, according to x-ray studies.[3] Raman and infrared vibrational spectroscopies have proved to be powerful tools to investigate the structure of this glass,[4] which presents extremely sharp peaks in the polarized Raman spectrum,[5] similar to other glasses, as SiO_2.[6] These sharp peaks in the Raman response have been explained in SiO_2 as symmetric vibrations of planar rings.[7]

The vibrations in pure B_2O_3 have been modeled before using a Born-type Hamiltonian with central and noncentral forces.[8] The amorphous network was simulated there by a Bethe lattice in which all boron atoms were forming boroxol rings. It was shown there that all the features measured in the infrared and Raman spectra could be identified, particularly those due to the vibrations of boroxol rings, which are extremely conspicuous. One important observation is that a noncylindrical angular force was needed to fit all the modes in the vibrational spectrum, and to agree with the experimental isotopic substitution shifts.[9]

The compound B_2O_3-xLi_2O is the basic substance to obtain a variety of fast-ion conducting glasses[10] in which the Li_2O acts as a modifier, changing the structure of the glass and producing a dramatic increase in the conductivity.[11] These structural changes are detected by NMR,[12] where the three-coordinated boron signal in boroxol rings disappears as x increases, and one perceives the appearance of regular local structures, as diborate, tetraborate, and metaborate complex groups. All these groups have at least one four-coordinated boron atom in a tetrahedral environment. When one is incorporating a proportion x of Li_2O into the B_2O_3 network, at least for small x, it is assumed[13] that for each Li atom added, a three-coordinated boron atom transforms into a four-coordinated charged atom, with the Li ion floating around, fairly free in the lattice. This assumption has been verified by ^{11}B NMR, where a one-to-one correspondence is obtained between the number of Li atoms and the number of four-coordinated borons, up to $x=40\%$.[14] This reaction has been described before,[10] and could be represented as in Fig. 1.

These structural changes can be detected by infrared and Raman spectroscopies. The vibrational signatures of these local complex groups produce changes in the spectra. These changes have been interpreted coherently,[10] although a theoretical calculation to attest this interpretation is lacking.

It is the purpose of this paper to develop a realistic and simple model to help in the interpretation of the Raman and infrared spectra. The basic idea is to build the simplest model that incorporates three important features: (1) The presence of tetrahedral boron sites, (2) the disorder, both topological and substitutional, and (3) the ac-

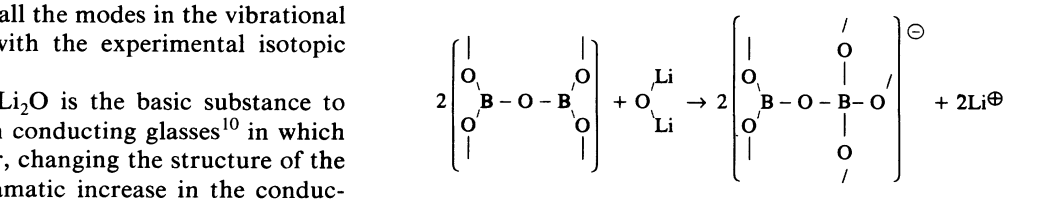

FIG. 1. Small amounts of Li_2O added to the B_2O_3 network. Each Li atom produces a negatively charged four-coordinated boron atom.

tivity of the different modes in the experiments. There is an interesting central-force model in a Bethe lattice of alternating three- and four-coordinated boron sites to study the changes in the vibrational bands,[15] and the results are encouraging. Here we propose an improvement to that model by taking into account noncentral forces, by incorporating substitutional disorder in the Bethe lattice [with a nested coherent-potential approximation (CPA) theory] and by applying a local polarizability model to calculate the spectral responses. The comparison with the experimental data is expected to be good only for $x \leq 40\%$, since it would be extremely cumbersome to treat intermediate range order structures, as diborates or tetraborates. For the same reason neither planar boroxol rings are considered.

In the following section, a detailed description of the formalism used is given, and expressions for the density of vibrational states (DOS), the Raman and infrared responses, as functions of x are found. In Sec. III, the results from the theory are exhibited and the interpretation of the experimental data is discussed in terms of the information provided by these results. In Sec. IV, we conclude and some comments about the validity of the results are presented.

II. THEORY

If one wants to investigate the changes in the vibrational response of vitreous B_2O_3 due to the presence of tetrahedral boron atoms, one could apply a bond CPA theory in a Bethe lattice. This sort of approach has proven useful in other amorphous alloys.[16] The basic CPA equations for the displacement-displacement Green's function $\mathbf{G}$ are

$$\underline{\mathbf{G}}_{A_i} = \sum_i P_{ij} \underline{\mathbf{G}}_{A_i B_j} , \tag{1}$$

where $\mathbf{G}_{A_i}$ is a 3×3 matrix for the displacements of an atom of type A_i embedded in an effective medium, $\mathbf{G}_{A_i B_j}$ is the Green's function of an atom with a bond of type ij in the same effective medium and P_{ij} is the probability of having such a configuration. The single line under the matrices means an average over all bonds, and the summation is over all possible bond configurations.

One can consider only boron-boron effective interactions. If one renormalizes the oxygen coordinates, there are only three possibilities for a bond, namely a three-coordinated atom ($B3$) bonded to a four-coordinated one ($B4$), a $B3$ to a $B3$ and a $B4$ to a $B4$. A convenient diagrammatic way of writing Eq. (1) is illustrated in Fig. 2, where the effective medium attached to a $B3$ atom is σ and the effective medium attached to a $B4$ atom is ξ. These two effective media need to be the same when the self-consistent solution is achieved, but it is convenient to consider them as different, in principle, to help a rapid convergence, this method is called nested CPA.[17] The probabilities P_{ij} of finding a given bond are written in terms of the amount x of Li_2O: If $\nu = x/(1+x)$, then $P_{i4} = \nu$ and $P_{i3} = 1-\nu$.

In order to be able to write the equations of Fig. 2, it is first necessary to eliminate the oxygen coordinates. We

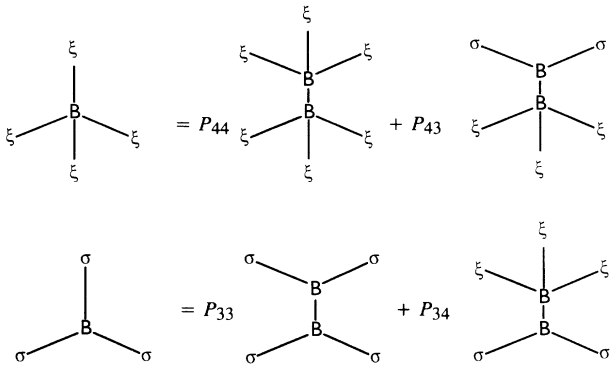

FIG. 2. Diagrammatic representation of the CPA equations for a disorder alloy with $B3$ and $B4$ atoms.

proceed following the method outlined in detail for the case of SiO_2,[18] and applied to the case of pure B_2O_3.[8] If one uses a Born-type Hamiltonian, the interaction between a $B3$ atom and an oxygen atom along a bond in the z direction is

$$\mathbf{D}_1 = \begin{pmatrix} \beta_x & 0 & 0 \\ 0 & \beta_y & 0 \\ 0 & 0 & \alpha \end{pmatrix} , \tag{2}$$

and if the bond is between a $B4$ and an oxygen, the interaction $\mathbf{D}_1'$ has the same form but the diagonal terms are β_x', β_y', and α'. Observe that the noncentral-force constants β need not be the same in both perpendicular directions. This generalization was made in pure B_2O_3 when the cylindrical symmetry of the bond is lost, as in the case of rings, or the $B3$ trigonal planar configuration. After eliminating the oxygens, the equation for the Green's function on a $B4$ atom (the first diagram on the left of Fig. 2) is

$$\mathbf{G}_{B4} = \left[M\omega^2 \mathbf{I} - \gamma' - \sum_{i=1}^{4} \langle \xi_i \rangle \right]^{-1} , \tag{3}$$

where the brackets $\langle \ldots \rangle$ mean a dihedral angle average,[18] M is the Boron mass, ω is the frequency, and $\mathbf{I}$ is the 3×3 identity matrix. The matrices along the tetradral directions i can be obtained from the ones along direction 1 by the proper rotations.[18] The self-energy term γ' must contain the oxygen coordinates

$$\gamma' = \sum_{i=1}^{4} \{ \mathbf{D}_i' + \langle \mathbf{D}_i' \mathbf{A}_i^{-1} \mathbf{D}_i' \rangle \} = \sum_i \{ \gamma_i' \} , \tag{4}$$

where the curly braces mean an average over configurations, that is, in terms of the concentration one has, for instance

$$\gamma_1' = \langle \nu(\mathbf{D}_1' + \mathbf{D}_1' \mathbf{A}_1^{-1}(44)\mathbf{D}_1') + (1-\nu)(\mathbf{D}_1' + \mathbf{D}_1' \mathbf{A}_1^{-1}(43)\mathbf{D}_1) \rangle , \tag{5}$$

where the matrices $\mathbf{A}$ contain the information about the

boron-boron bond through an oxygen atom, and they could be of four types: $B4$-$B4$, $B4$-$B3$, $B3$-$B4$, and $B3$-$B3$, and along a $B4$-O bond in the z direction they are explicitly

$$\begin{aligned}
\mathbf{A}_1(44)&=m\omega^2\mathbf{I}-\mathbf{D}_1'-\Theta^{-1}\mathbf{D}_1'\Theta\ ,\\
\mathbf{A}_1(43)&=m\omega^2\mathbf{I}-\mathbf{D}_1'-\Theta^{-1}\mathbf{D}_1\Theta\ ,\\
\mathbf{A}_1(34)&=m\omega^2\mathbf{I}-\mathbf{D}_1-\Theta^{-1}\mathbf{D}_1'\Theta\ ,\\
\mathbf{A}_1(33)&=m\omega^2\mathbf{I}-\mathbf{D}_1-\Theta^{-1}\mathbf{D}_1\Theta\ ,
\end{aligned} \tag{6}$$

where m is the oxygen mass, Θ is a rotation on the x axis by $\theta=130°$, which is considered fixed for all B-O-B bonds, since all the oxygens are bridging atoms and there is very little dispersion of this angle in the glass. As an example, the Green's function corresponding to the diagram occurring with probability P_{43} in Fig. 2 is

$$\mathbf{G}_{B4B3}=\left[M\omega^2\mathbf{I}-\mathbf{R}_4-\sum_{i\neq 1}^{4}\langle\xi_i\rangle-\langle\mathbf{D}_4(M\omega^2\mathbf{I}-\mathbf{R}_3-\sum_{j\neq 1}^{3}\sigma_j)^{-1}\mathbf{D}_4^{*}\rangle\right]^{-1}, \tag{7}$$

where the $B4$ atom is linked to a $B3$ atom through bond 1. The effective interaction through that bond is

$$\mathbf{D}_4=\mathbf{D}_1'\mathbf{A}_1(43)^{-1}\Theta^{-1}\mathbf{D}_1 \tag{8}$$

and

$$\mathbf{D}_4^{*}=\mathbf{D}_1\Theta\mathbf{A}_1(34)^{-1}\mathbf{D}_1'\ .$$

The self energies for both atoms are

$$\begin{aligned}
\mathbf{R}_4&=\gamma'-\gamma_1'+\mathbf{D}_1'+\mathbf{D}_1'\mathbf{A}_1(43)^{-1}\mathbf{D}_1\ ,\\
\mathbf{R}_3&=\gamma-\gamma_1+\mathbf{D}_1+\mathbf{D}_1\Theta\mathbf{A}_1(34)^{-1}\Theta^{-1}\mathbf{D}_1'\ ,
\end{aligned} \tag{9}$$

where the averaged self-interaction γ has the three bonds on the trigonal directions, obtained by rotations around the x axis by $2\pi/3$. Thus

$$\gamma=\sum_{i=1}^{3}\{\gamma_i\}\ ,$$

where,

$$\gamma_1=\langle\nu(\mathbf{D}_1+\mathbf{D}_1\mathbf{A}_1(34)^{-1}\mathbf{D}_1')+(1-\nu)(\mathbf{D}_1+\mathbf{D}_1\mathbf{A}_1(33)^{-1}\mathbf{D}_1)\rangle\ . \tag{10}$$

The diagrams in Fig. 2 represent a complete set of equations for ξ or σ, which is solved self-consistently, to a desired percent accuracy (10^{-5} in our case), for the maximum difference between matrix elements. This effective medium, σ or ξ, represents a Bethe lattice containing the disorder, which can be used to calculate any quantity of interest, besides the self-correlations at the boron sites. For instance, one can find the local vibrations of a mass $\mathbf{m}$, at an oxygen site linking a $B3$ with a $B4$, by

$$\mathbf{G}_{34}^{0}=\langle(\mathbf{A}_1(34)-\mathbf{D}_1\mathbf{Z}_{31}^{-1}\mathbf{D}_1-\Theta^{-1}\mathbf{D}_1'\mathbf{Z}_{41}^{-1}\mathbf{D}_1'\Theta)^{-1}\rangle\ , \tag{11}$$

where,

$$\mathbf{Z}_{41}=\left\langle m\omega^2\mathbf{I}-(\gamma'-\gamma_1')-\mathbf{D}_1'-\sum_{i\neq 1}^{4}\xi_i\right\rangle \tag{12}$$

and

$$\mathbf{Z}_{31}=\left\langle m\omega^2\mathbf{I}-(\gamma-\gamma_1)-\mathbf{D}_1-\sum_{j\neq 1}^{3}\sigma_j\right\rangle\ . \tag{13}$$

In this way, one could find the self-correlations at all local atomic configurations. There are two possible configurations for the boron atoms, and three configurations for the oxygen atoms. If one defines the local DOS for each configuration as

$$\rho_i=\frac{-2M\omega}{\pi}\,\mathrm{Im}(\,\mathrm{Tr}\mathbf{G}_i),\quad\text{and}\quad\rho_{ij}^{0}=\frac{-2m\omega}{\pi}\,\mathrm{Im}(\,\mathrm{Tr}\mathbf{G}_{ij}^{0})\ , \tag{14}$$

then, the averaged total DOS is

$$\rho^{T}=\frac{[2-\nu][(1-\nu)\rho_{B3}+\nu\rho_{B4}]+[3-\nu][(1-\nu)^2\rho_{33}^{0}+2\nu(1-\nu)\rho_{34}^{0}+\nu^2\rho_{44}^{0}]}{(5-2\nu)}\ . \tag{15}$$

In order to compare the results with the experiments, one needs a model for the Raman and infrared spectral responses. Since this oxide presents a highly polarized Raman spectrum, one is able to use the local polarizability model applied to SiO_2.[18] The approximate expression for the polarized part of the Raman spectrum is proportional to

$$-\omega\,\mathrm{Im}\left[\sum_{\alpha\beta}\sum_{ll'}v_\alpha(l)\mathbf{G}_{\alpha\beta}(l,l')v_\beta(l')\right], \tag{16}$$

where $v_\alpha(l)$ is the α component of the sum of the unit vectors along *all* the bonds arriving at site l, therefore, it is not nil only if the site is in a nonsymmetric environment. Equation (16) will emphasize the symmetric stretching modes at the oxygen sites. Furthermore, in Ref. 18 is shown that the infrared response is related to the imaginary part of the complex dielectric function ε, and it could be written as

$$\omega\varepsilon_2=-\omega\,\mathrm{Im}\,\mathrm{Tr}\left[\sum_{ll'}e(l)\mathbf{G}(l,l')e(l')\right], \tag{17}$$

where the dynamical charge tensor e has been approximated by isotropic point charges, -2 in the oxygen sites and $+3$ and $+4$ in the $B3$ and $B4$ sites, respectively. To

calculate Eqs. (16) and (17), one needs to perform a summation over all sites, which gives spurious results in the Bethe lattice.[19] Therefore, we applied the local approximation used in Ref. 18, calculating the spectral responses in clusters consisting of a central boron site and its neighbor boron atoms. There are nine different local configurations: If the central site is a $B3$, the three neighbors could be $B3$ or $B4$, giving four, and if the central site is $B4$, the possible combinations of the four neighbors give another five. The weighted average of all clusters with a $B4$ atom at the center defines a 15×15 matrix

$$\Gamma_4=\begin{vmatrix} \mathbf{D}'_0 & \mathbf{D}'_1 & \mathbf{D}'_2 & \mathbf{D}'_3 & \mathbf{D}'_4 \\ \mathbf{D}'_1 & \mathbf{Q}'_1 & 0 & 0 & 0 \\ \mathbf{D}'_2 & 0 & \mathbf{Q}'_2 & 0 & 0 \\ \mathbf{D}'_3 & 0 & 0 & \mathbf{Q}'_3 & 0 \\ \mathbf{D}'_4 & 0 & 0 & 0 & \mathbf{Q}'_4 \end{vmatrix}^{-1} , \tag{18}$$

where $\mathbf{D}'_0$ is the self-energy of the central site, namely,

$$\mathbf{D}'_0=M\omega^2\mathbf{I}-\sum_{i=1}^{4}\mathbf{D}'_i , \tag{19}$$

and the other diagonal blocks are the self-energies of the outer boron atoms. Care has to be taken to make the appropriate averages, first of all, each $\mathbf{Q}'_i$ could be either

$$\mathbf{q}_{3i}=\Phi_i^{-1}[m\omega^2\mathbf{I}-\mathbf{D}'_i-\Theta\mathbf{D}_i\Theta^{-1}-\Theta^{-1}\mathbf{D}_i\mathbf{Z}_{3i}^{-1}\mathbf{D}_i\Theta]\Phi_i , \tag{20}$$

if there is a $B3$ atom through bond i, or, if the atom is $B4$, then

$$\mathbf{q}_{4i}=\Phi_i^{-1}[m\omega^2\mathbf{I}-\mathbf{D}'_i-\Theta D'_i\Theta^{-1}-\Theta^{-1}\mathbf{D}'_i\mathbf{Z}_{4i}^{-1}\mathbf{D}'_i\Theta]\Phi_i , \tag{21}$$

where Φ_i is a rotation around the z_i axis by a random angle ϕ. Therefore,

$$\begin{aligned} \mathbf{Q}'_1&=(1-\nu)^4\mathbf{q}_{31}+\mathbf{q}_{41}-(1-\nu)^4\mathbf{q}_{41} , \\ \mathbf{Q}'_2&=[\nu^4+4\nu^3(1-\nu)+6\nu^2(1-\nu)^2]\mathbf{q}_{32} \\ &\quad+[4\nu(1-\nu)^3+(1-\nu)^4]\mathbf{q}_{42} , \\ \mathbf{Q}'_3&=[\nu^4+4\nu^3(1-\nu)]\mathbf{q}_{33} \\ &\quad+[6\nu^2(1-\nu)^2+4\nu(1-\nu)^3+(1-\nu)^4]\mathbf{q}_{43} , \\ \mathbf{Q}'_4&=\nu^4\mathbf{q}_{34}+[4\nu^3(1-\upsilon)+6\nu^2(1-\nu)^2 \\ &\quad+4\nu(1-\nu)^3+(1-\nu)^4]\mathbf{q}_{44} . \end{aligned} \tag{22}$$

There are similar equations defining 12×12 matrices representing the clusters with a $B3$ atom as a central site (Γ_3). With these definitions, Eqs. (16), (17), and (18) depend on the random angles ϕ chosen in each rotation, in order to simulate the complete randomness of dihedral angles, we averaged over 20^4 independent rotations. The final Raman response is

$$-\omega\,\mathrm{Im}(\upsilon\langle v_4^T\Gamma_4 v_4\rangle+(1-\nu)\langle v_3^T\Gamma_3 v_3\rangle) , \tag{23}$$

where the brackets mean the ϕ average and the subindexes refer to the central site of the clusters. Analogously, the infrared response is

$$-\omega\,\mathrm{Im\,Tr}(\nu\langle e_4^T\Gamma_4 e_4\rangle+(1-\nu)\langle e_3^T\Gamma_3 e_3\rangle) . \tag{24}$$

III. RESULTS

Equations (14) represent a rather involved calculation, with several averages, two nested self-consistent loops and various parameters, therefore it is necessary to test the theory in known limiting cases. When $x=0$ and $\beta_i=0$, the theory reproduces the allowed bands predicted by a network dynamics model.[20] Furthermore, with central forces only, and $\nu=0.5$ the bands in the DOS follow closely the results by Deppe, Balkanski, and Wallis[15] except that the graphs are somewhat smeared out by the disorder. This comparison helped us to fix the value of α', since they obtained better results for a ratio $\alpha/\alpha'=0.8$, and α should be near their value of 470 N/m when noncentral forces are added. The other limit, when $x=\infty$, or $\upsilon=1$, was tested by reproducing the results for AX_2 glasses with the appropriate parameters[18] for SiO_2 and GeO_2. In this case we were able to reproduce not only the local DOS but also the Raman and infrared responses.

Figure 3 shows the total DOS from Eq. (15) for various values of x, chosen to be the same as the experimental

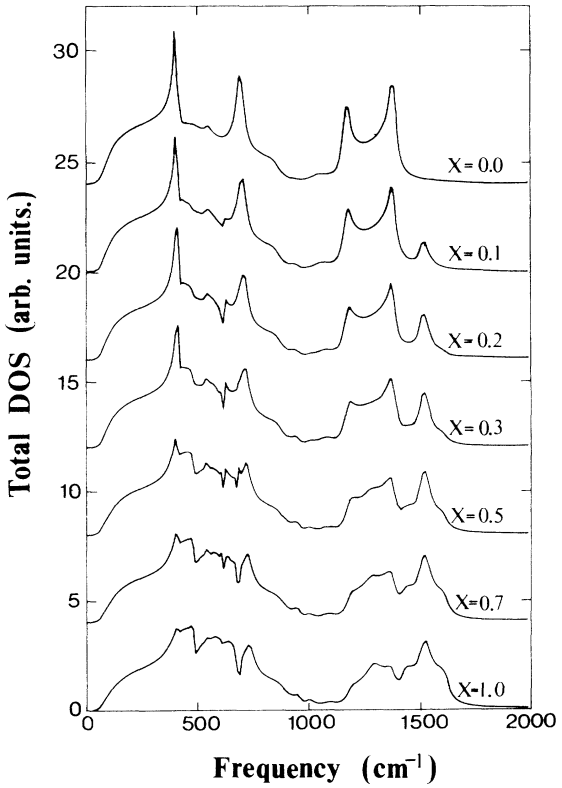

FIG. 3. Total density of vibrational states of B_2O_3-$x\,Li_2O$, as a function of x. A small imaginary part of 20 cm^{-1} was added to the frequency in all graphs.

TABLE I. Parameters used in the calculations.

Force constants (N/m)								
α	β_x	β_y	α'	β'_x	β'_y	θ	m (au)	M (au)
430	80	82	567	146	146	130°	16	10.8

data by Massot and Balkanski.[11] The parameters used are the ones in Table I, and were fitted to obtain a spectrum similar to Fig. 6 of Ref. 8 for $x=0$. For $x=0$, there is a low-frequency band with two main features at ~ 400 and 700 cm^{-1}, with a valley in between, and a high-frequency band with two peaks, all of this in close resemblance with Fig. 6(a) of Ref. 8. The sharp peak at 808 cm^{-1} is not seen here because of the absence of boroxol rings in the calculation. As the amount of Li is increased, new features appear, particularly in the region of the valley and in the high-frequency edge, due to stretching of tetrahedral units. The main features, as the gap and the band limits are accurately reproduced. The primed β parameters for $B4$ cannot be obtained with this fitting, although there must be the same in the x and y directions in a tetrahedral symmetry. Their actual value was chosen by fitting the high-frequency part of the infrared response.

Figure 4 shows the local DOS at the $B4$ and $B3$ sites. The plot for $x=0$ at a $B4$ site corresponds to a single $B4$ impurity embedded in a B_2O_3 matrix. Observe that the vibrations of a $B4$ atom reach higher frequencies, which is seen in the experiment, and that the bending modes at ~ 760 cm^{-1} are extremely sharp and disappear very rapidly with x. The modes at a $B3$ site are modified with x mainly in the middle region of the spectrum. These correspond to the part in which the various O-B bonds induce disorder, as can be corroborated in the local DOS at the three types of oxygen sites, which are shown in Fig. 5.

Observe that the bands of the $O44$ unit are more affected by disorder, and many fluctuations appear due to the difficulty of accommodating these bonds in the network. Also, observe that the sharp peak at 620 cm^{-1} in the $B4$ site contains a lot of oxygen motion; this means that the bending modes of the tetradral units are extremely localized.

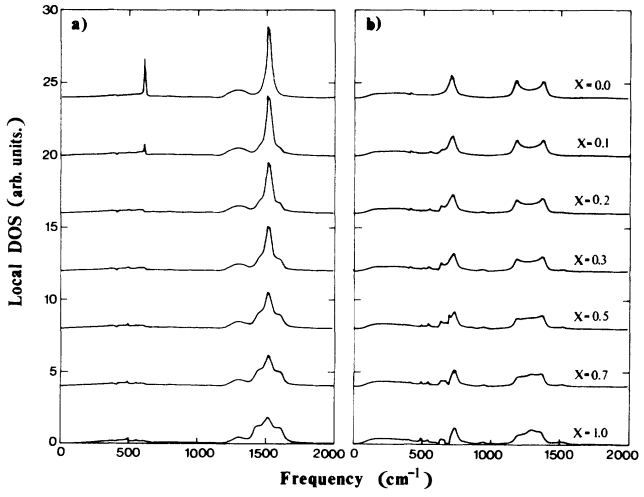

FIG. 4. Local density of vibrational states at (a) a four-coordinated boron site $B4$ and (b) at a three-coordinated $B3$ site, as a function of x.

The calculated Raman response is presented in Fig. 6. Let us discuss first the $x=0$ spectrum. There are three main regions, also seen in the experiment:[10] A wide band centered at ~ 500 cm^{-1}, a peak at 808 cm^{-1}, and a less intense band at around 1300 cm^{-1}. The first corresponds to in-phase oxygen motion, the peak at 808 cm^{-1} is not as sharp and intense as in the experiment, because this is attributed to a breathing mode of the boroxol rings, not included in the theory, nevertheless, with the help of Figs. 4 and 5, we could say that at this frequency there is mostly oxygen motion. The higher frequency band has optical modes involving a lot of boron motion and stretching of bonds. The fluctuations in the low-frequency shoulder are due to the ϕ average and could be removed by increasing the number of random clusters in the average. We did not worry about this because we are interested in frequencies greater than 500 cm^{-1}.

When x is increased, four main effects are seen in the experiment: (1) The band at 500 cm^{-1} is almost not affected and there is a shift of the maximum to higher frequencies, (2) the peak at 808 cm^{-1} gradually disappears without shifting, (3) a couple of new peaks appear at ~ 760 and 960 cm^{-1}, and (4) the intensity of the high-frequency modes is increased. The same trends are seen in the present calculation, in almost quantitative agreement with the experiment. The main source of discrepancy is the absence of boroxol rings in the calculation, which deters the appearance of the highly polarized sharp peak. It is convenient to remember that one should not expect agreement in the relative intensities of the peaks from this very simple local polarizability model.

Figure 7 shows the results of the infrared response. Here the intensities should be completely wrong, but the frequencies of the active modes should be correct. The pure glass result presents the usual to bands, at around 720 and 1360 cm^{-1}, the low-frequency one does not shift with x, and the other one decreases its relative intensity when increasing x. A new band appears at frequencies >1500 cm^{-1}, due to the $B4$ units. All this is also seen in the experiment, however, there is some disagreement because in the experiment there is a conspicuous band centered at 1000 cm^{-1}, not seen in the calculation. This latter band is attributed in Ref. 10 to a stretching motion in the tetrahedral $B4$ units, which are in diborate and tetraborate groups. These groups are absent in this theory and we attribute this disagreement mainly to this circumstance. We support this by the fact that the infrared response of polycrystalline lithium diborate is principally in the region between 800 and 1100 cm^{-1} (Fig. 11 in Ref. 10).

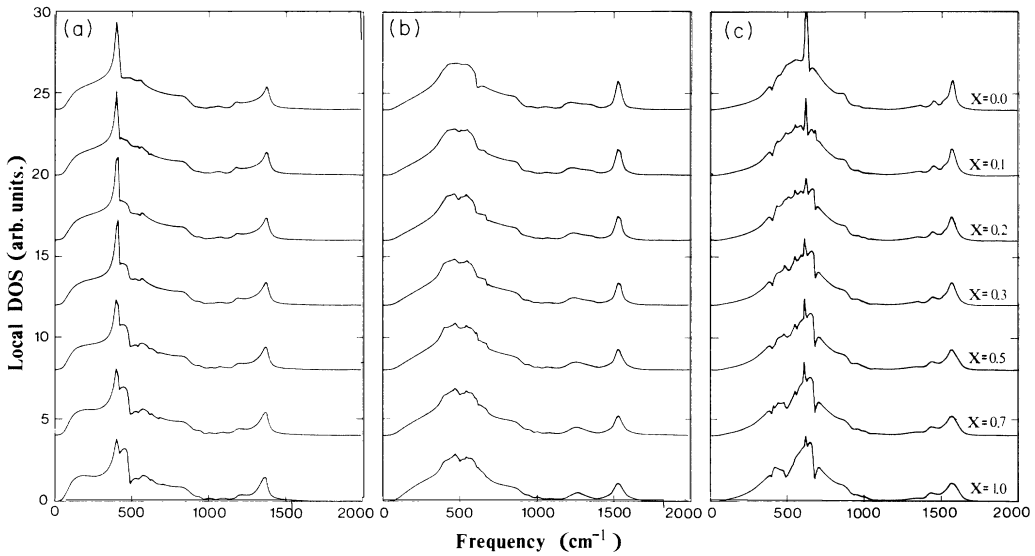

FIG. 5. Local density of vibrational states at the three different oxygen sites. (a) at a $O33$ site, (b) at a $O34$ site, and (c) at a $O44$ site.

One should mention that when $x > 0.3$ there is the evidence that nonbridging oxygen atoms are present in the glass. The stretching vibrations of these atoms are expected to be around 980 cm^{-1}, and are very strongly infrared active. None of these effects are contemplated in the present theory, although it would be relatively simple to incorporate nonbridging atoms.

IV. CONCLUSIONS

We have presented a formalism to calculate the vibrational response of boron oxide with an alkali-metal oxide

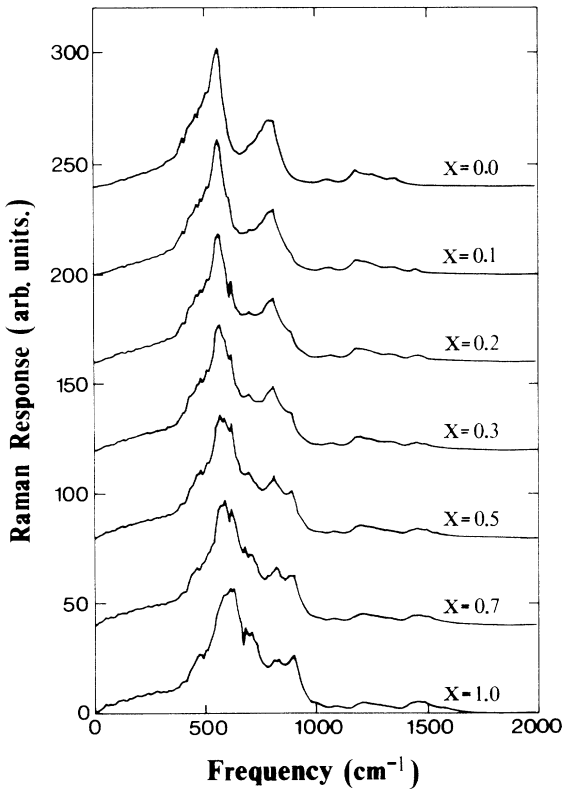

FIG. 6. Raman Spectrum calculated from Eq. (23) as a function of x. The cluster average included 700 different calculations at each frequency (intervals of 10 cm^{-1}).

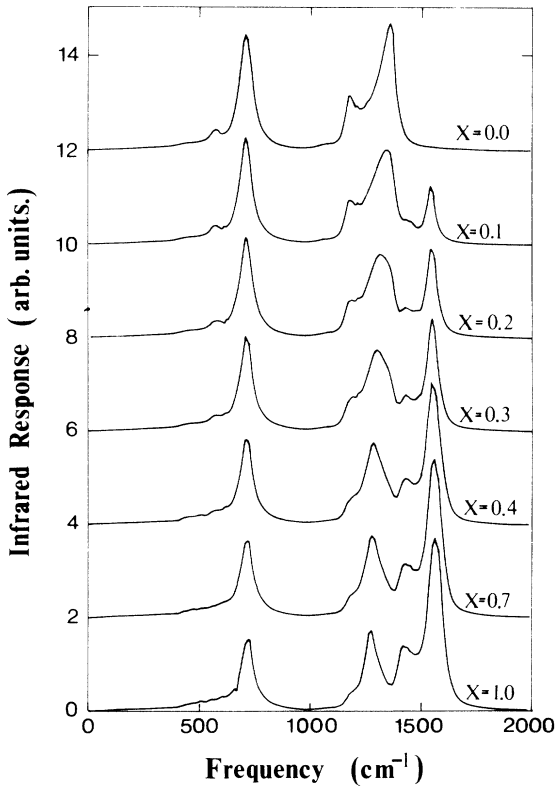

FIG. 7. Infrared spectrum calculated with Eq. (24) as a function of x. Isotropic charge tensors for completely ionic bonds were used in the calculation.

modifier. The theory incorporates important features, as the alloylike disorder and the main structural change that the modifier produces. The results are in agreement with the experimental data available and confirm the presence of tetrahedral $B4$ units in the doped material. In spite of the simplicity of the theory, most of the features in the experimental spectra are readily seen in the theoretical calculations.

The local DOS at the various sites permit a further insight into the nature of the vibrations in any particular region of the spectra, and substantiate the former assignations to the experimental peaks, particularly those due to the $B4$ units.

The main shortcoming of the theory is the absence of planar boroxol rings, which are the most abundant structures in B_2O_3. Neither the appearance of metaborates, complex diborate or tetraborate structures is included. At present, a CPA calculation of this sort with clusters of several dozens of atoms and several hundreds of configurations is exceedingly demanding, and we believe is not worth pursuing at the moment. It is rewarding to obtain so many points of agreement with the experiment with such a little computational effort.

ACKNOWLEDGMENTS

We are pleased to thank M. Balkanski, Roger Elliott, and J. Deppe for helpful discussions and encouragement as part of the joint program supported by the Commission of the European Communities, through Contract No. CL1-CT90-0864 (DSCN). We are grateful to F. Galeener and J. Avendaño for valuable help. Partial support from Comisión de Fomento de las Actividades Académicas-Instituo Politécnico Nacional to F.L.C.A. and from Dirección General de Asuntos del Personal Académico-Universidad Nacional Autónoma de México is acknowledged.

[1]J. Goubeau and H. Z. Keller, Inorg. Chem. **272**, 303 (1953); J. Krogh-Moe, J. Non-Cryst. Solids **1**, 269 (1969).

[2]G. E. Jellison, Jr., L. W. Panek, P. J. Bray, and G. B. Rouse, Jr., J. Chem. Phys. **66**, 802 (1977).

[3]R. L. Mozzi and B. E. Warren, J. Appl. Crystallogr. **3**, 251 (1970).

[4]F. L. Galeener, G. Lucovsky, and J. C. Mikkelsen, Jr., Phys. Rev. B **8**, 3983 (1980).

[5]D. L. Griscom, in *Borate Glasses,* edited by L. D. Pye, V. D. Frechette, and N. J. Kreidl (Plenum, New York, 1978).

[6]F. L. Galeener, Solid State Commun. **44**, 1037 (1982).

[7]F. L. Galeener, R. A. Barrio, E. Martinez, and R. J. Elliott, Phys. Rev. Lett. **53**, 2429 (1984).

[8]R. A. Barrio, F. L. Castillo-Alvarado, and F. L. Galeener, Phys. Rev. B **44**, 7313 (1991).

[9]F. L. Galeener and A. E. Geissberger, J. Phys. (Paris) **C9**, 343 (1982).

[10]M. Massot, M. Balkanski, and A. Levasseur, in *Microionics, Solid State Integrable Batteries,* edited by M. Balkanski (North-Holland, Amsterdam, 1991), p. 139.

[11]M. Massot and M. Balkanski, in *Disorder in Condensed Matter Physics,* edited by J. Blackman and T. Tagüeña (Clarendon, Oxford, 1991), p. 74.

[12]P. J. Bray, A. E. Geissberger, F. Bucholtz, and I. A. Harris, J. Non-Cryst. Solids **52**, 45 (1982).

[13]W. L. Konijnendijk, Phillips Res. Rep., Suppl. 1 (1975); see also Ref. 3.

[14]P. J. Bray, S. A. Feller, G. E. Jellison, Jr., and Y. H. Yun, J. Non-Cryst. Solids **38/39**, 98 (1980).

[15]J. Deppe, M. Balkanski, and R. F. Wallis, Phys. Rev. B **41**, 7767 (1990).

[16]F. L. Castillo-Alvarado, G. S. Contreras-Puente, and R. A. Barrio, J. Phys. C **21**, 1887 (1988).

[17]J. Avendaño, F. L. Castillo-Alvarado, and R. A. Barrio, J. Non-Cryst. Solids, **137&138**, 299 (1991).

[18]R. A. Barrio, F. L. Galeener, and E. Martínez, Phys. Rev. B **31**, 7779 (1985).

[19]F. Yndurain, R. A. Barrio, R. J. Elliott, and M. F. Thorpe, Phys. Rev. B **28**, 3576 (1983).

[20]F. L. Galeener and M. F. Thorpe, Phys. Rev. B **28**, 5802 (1983).